WILLIAM & MARY
CHARTERED 1693

W&M ScholarWorks

Undergraduate Honors Theses

Theses, Dissertations, & Master Projects

5-2019

The use of foundational mathematical modeling techniques to inform understanding & design of complex biological systems

Callan Monette

Follow this and additional works at: https://scholarworks.wm.edu/honorstheses

Part of the Biotechnology Commons, Ordinary Differential Equations and Applied Dynamics Commons, and the Systems Biology Commons

The use of foundational mathematical modeling techniques to inform understanding & design of complex biological systems

A thesis submitted in partial fulfillment of the requirement

for the degree of Bachelor of Science in Computational & Applied Mathematics & Statistics from

The College of William and Mary .

by

Callan Monette

Accepted for _Honors_

Dr. Margaret Saha, Director

Dr. Eric Bradley

Dr. Gregory Conradi Smith

Dr. Mark Forsyth

Williamsburg, VA

May 3, 2019

INTRODUCTION

Synthetic biology is a relatively new and diverse field with the potential to revolutionize our command over biological systems via the modification or de novo construction of biological networks and to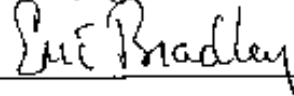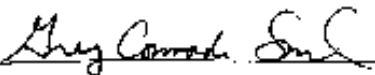ols. Precise and predictable control over the foundational properties of gene expression and genetic circuit behavior will be critical to the application of synthetic biology in the relevant contexts (for instance, *in vivo* for therapeutic applications). This level of control can be achieved via the interplay between mathematical modeling and empirical observation. The following work will highlight not only the massive potential of synthetic biology in both bacterial and mammalian systems, but the essential role of mathematical modeling in the field to understand existing biological systems and inform the design of novel systems to control biology. I will also outline my efforts to expand the capabilities of synthetic biology research at William & Mary to include work in mammalian systems, creating a sustainable and accessible framework to enable future students to delve into fundamental control of biological systems on the cutting edge of mammalian synthetic biology research.

CHAPTER 1: DEGRADATION-BASED CONTROL OF GENE EXPRESSION RESPONSE TIME

Background

One of the primary goals of synthetic biology is to create biological tools which can be used in a modular, plug-and-play fashion to predictably tune gene and genetic circuit behavior. To that end, the field has developed a massive and diverse assortment of well-characterized tools which provide a high level of control over static, or steady state, properties of circuit behavior. For instance, precise control over gene expression magnitude is obtainable by utilizing one of a

series of well-characterized promoters or ribosome binding sites (RBSs) (Kelly et al., 2009), and genetic switches and logic gates can be constructed on the basis of whether a series of genes are "on" or "off" when the system is at steady state (Anderson, Voigt, & Arkin, 2007; Nielsen et al., 2016; Siuti, Yazbek, & Lu, 2013). As the field delves deeper into controlling and designing novel complex biological systems, it has become clear that the highly dynamic nature of cellular signal processing demands a move beyond the steady state properties of a system and into deeper consideration of the dynamic aspects of gene expression. The ability to precisely control gene expression dynamics at a basic level, with a collection of simple and modular tools comparable to those available for steady state properties, would therefore be instrumental in elucidating new understanding of dynamic signal processing and enabling a new dimension of control over biological systems.

One fundamental property of gene expression dynamics is response time, or the time taken for gene expression output to reach its steady state. Notably, control over gene expression response time has been achieved in the past via post-translational modification (Gordley et al., 2016) and circuit redesign to incorporate additional feedback interactions such as negative autoregulation (Maeda & Sano, 2006; Rosenfeld, Elowitz, & Alon, 2002). However, it would be particularly useful to predictably control response time with the simple insertion a single genetic part, much like the insertion of a particular ribosome binding site confers a predictable change in gene expression magnitude at steady state. This type of genetic part-level control would be ideal in the interest of speeding up a given circuit's output response without redesigning the architecture of the circuit itself.

Here we present a simple, modular, accessible framework for the control of gene expression response time based on a mathematical model which predicts a relationship between

response time and protein degradation. We demonstrate that protein degradation can be used to control response time in a predictable manner based on this model, and that output steady state can be manipulated independently of this response time change. Finally, we investigate the control of response time in the context of an incoherent feedforward loop, a more complex circuit architecture which generates a pulse output, to demonstrate that this framework could be applied to control circuit dynamics beyond simple response time.

Mathematical model

The basis of this framework is a simple mathematical model described by Uri Alon which is used to describe the output over time of an inducible gene (Alon, 2006). As seen in Equation 1, the change in output protein concentration (x) over time is based on the production and degradation We can represent the production and degradation rates for the output protein using lumped parameters to create a simple and generalizable model as seen in Equation 1.

$$\frac{dx}{dt} = \alpha - \gamma x \qquad (1)$$

The production rate for our protein is represented by α, encompassing both transcription and translation rates. Likewise, the parameter γ combines both degradation rate and dilution due to cell division.

By solving Equation 1 we can determine the concentration of protein x for a given time t in terms of the above production and degradation parameters:

$$x(t) = \frac{\alpha}{\gamma}\left(1 - \frac{1}{e^{\gamma t}}\right) \qquad (2)$$

This equation is characterized by an exponential relaxation up to some constant protein

concentration, known as steady state, at the value $\frac{\alpha}{\gamma}$. Since the function approaches steady state

asymptotically, we choose $\tau_{1/2}$, the time taken to reach half of steady state, as a metric for gene

expression response time. Solving for this metric, we find:

$$\tau_{1/2} = \frac{\ln(2)}{\gamma} \qquad (3)$$

The implication of this solution is that control over degradation alone can be used to control

response time, defined here as time to half of steady state; furthermore, we predict an inverse

relationship between response time and degradation rate.

Degradation-Based Framework for Response Time Control

In order to gain tunable, genetic part-based control over gene expression response time,

we chose to utilize a collection of modular protein degradation tags (pdts) which was designed

and characterized by the Collins lab in 2014 (Cameron & Collins, 2014). Each 27 amino acid

tag, when added to the C-terminus of a protein of interest, is recognized and targeted by the mf-

Lon protease for degradation. Notably, this protease is native to the *Mesoplasma florum* bacteria

and has been shown to act orthogonally to *E. coli*-native protease systems; in other words, *E. coli*

endogenous proteases do not recognize Collins' pdts, and mf-Lon does not recognize native *E.

coli* tags (Gur & Sauer, 2008). We chose 5 pdts with distinct protease affinities, hoping to

achieve distinct response times and predicting that insertion of tags with a higher protease

affinity would yield a higher degradation rate and therefore confer a more rapid expression

response time.

In order to create and test this framework, we utilized a series of inducible reporter constructs, each consisting of the mScarlet-I fluorescent protein tagged with a pdt under the control of an anhydrous tetracycline (ATc)-inducible promoter. The inducible reporter constructs were cloned onto high-copy plasmid backbones and co-transformed with the gene for the mf-Lon, which was placed under the control of an Isopropyl β-D-1-thiogalactopyranoside (IPTG)-inducible promoter and cloned onto a low-copy plasmid. To measure response time, time-course experiments were conducted over 4 hours, with fluorescence measurements taken using fluorescence-activated cell sorting (FACS) every 20 minutes. A full account of experimental methods and construct design can be found in Appendix I.

In the interest of expanding our work to include a more complex dynamic behavior beyond simple response time, we investigated dynamic control in the context of the pulse-generating circuit architecture known as an incoherent feedforward loop (IFFL). This circuit consists of the simultaneous activation of both an output and a repressor for the output. The delayed repression of the output leads to an initial rapid increase in output concentration followed by a sharp decrease once the repressor takes effect, creating a pulse. We were able to recreate this circuit architecture within the pdt/mf-Lon framework by simultaneously inducing our output reporter and the mf-Lon protease which targets the tagged output protein. Within this framework, we expected the affinity of the pdt with the protease to correlate to the sharpness of the pulse produced by the IFFL.

Results

We found that as expected, the inducible reporter expression did display response times that were dependent upon the tag strength (Figure 1a). Since our time course experiments were conducted in the context of the IFFL circuit, with simultaneous induction of our reporter and mf-

Lon constructs, we were able to go beyond response time analysis and further found that the sharpness of the pulse generated by the IFFL was also dependent on the strength of the pdt used (Figure 1b).
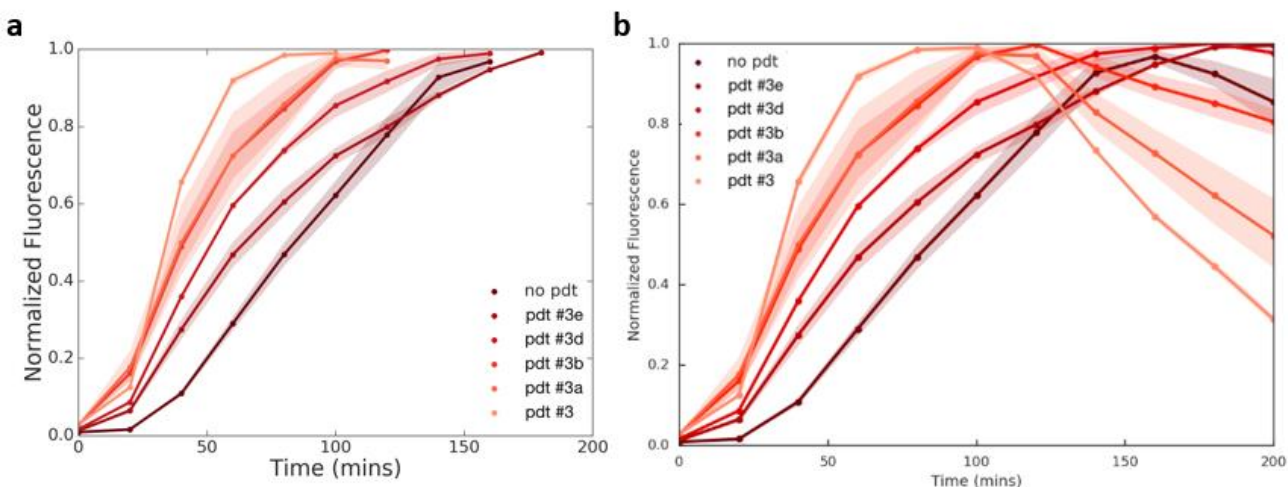

Figure 1: (a) Time course measurements for absolute fluorescence (MEFL) of ATc inducible reporter + pdt constructs; pdts are listed in order of increasing protease affinity. These measurements are normalized to their steady state value and, for clarity of response time visualization, traces are truncated once steady state (defined as the time point at which the two following measurements were not above the value of that time point) is reached. (b) Untruncated time courses to enable visualization of the full pulsatile output generated by the IFFL circuit architecture. For (a) and (b), each data point represents the geometric mean of 10,000 or more single cell measurements taken via flow cytometry of three biological replicates. Shading represents +/- one geometric standard deviation from the mean.

We also sought to determine whether the degradation-dependent change in response time followed the inverse mathematical relationship predicted by the model. We determined relative degradation rates for each pdt by taking the ratio of their final, steady state fluorescence relative to the untagged control (Figure 2a). We then plotted these relative degradation rates against the

response time for each pdt as well as for a tagless control (Figure 2b). We found that relative

degradation rate and response time do indeed display an inverse scaling relationship, as predicted

by the mathematical model.
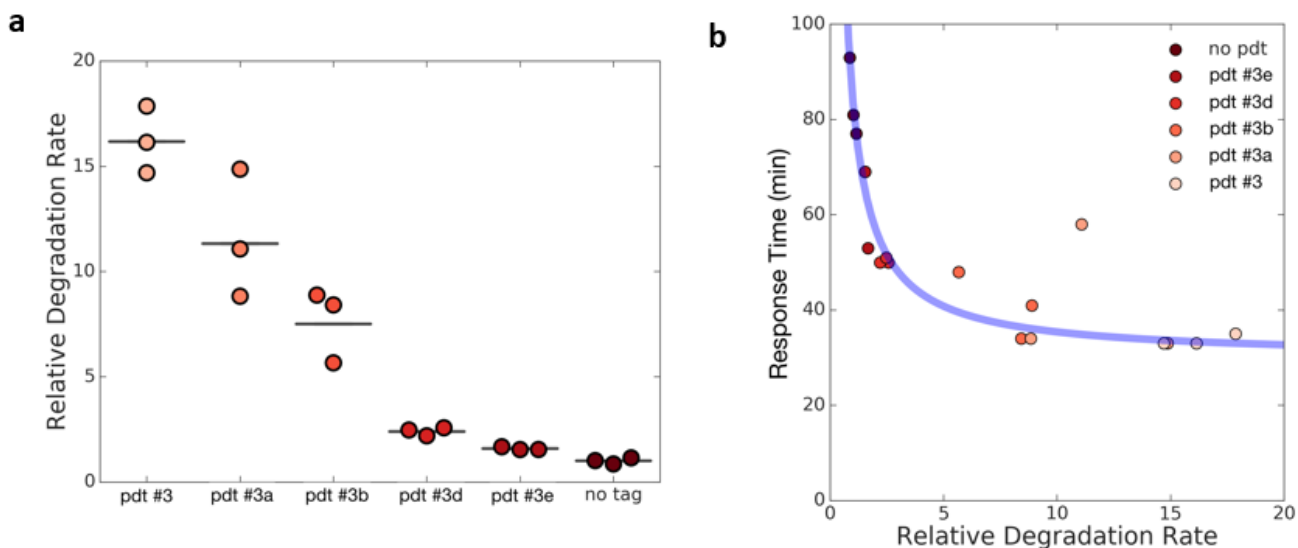
Figure 2: (a) Relative degradation rates for each of the pdt reporter constructs, determined by

taking the steady state fluorescence relative to untagged fluorescence. Each data point

represents the population geometric mean of at least 10,000 cells for a biological replicate; the

line represents the geometric mean of the three replicates. (b) Plot of relative degradation rate

versus response time in minutes. The blue line represents a guide to the eye demonstrating an

inverse relationship between the two variables.

Discussion

While our work empirically demonstrates an inverse scaling relationship between gene

expression response time and relative degradation rate, we wanted to ensure that pdts could be

useful in controlling the response time of an existing arbitrary circuit. One notable consequence

of increasing degradation rate via pdts in order to control response time is that the steady state

output concentration decreases. However, given that steady state is defined according to our

model by production rate over degradation rate, we find that steady state concentration can be readjusted to its original value by increasing production rate. Furthermore, since our model dictates that degradation rate alone contributes to the gene expression response time, we expect that changes to production rate will not affect the change in response time. As a proof of concept, we successfully achieved this effect for one of the pdts, increasing production rate by increasing inducer concentration to readjust steady state back to its original tag-free value (Appendix II).

One notable limitation of our framework is the potential for toxicity associated with the expression of the mf-Lon protease. Although the protease was determined to be orthogonal to *E. coli*'s endogenous protein degradation systems (Gur & Sauer, 2008), empirically we experienced problems with cell toxicity. We found that the expression of the protease construct on a medium- to low-copy plasmid alleviated this toxicity to some extent; however, expression of this construct over a period of hours remained problematic. For this reason, response time measurements were primarily taken in the context of the IFFL circuit, with simultaneous induction of our reporter and protease constructs. While ideally, a response time control demonstration could be achieved with induction of our reporter occurring while the protease is already at steady state, we are continuing work to obtain reliable data through this method by adjusting induction conditions. Ultimately, the results obtained via simultaneous induction provide a proof-of-concept of response time control via modular control of degradation rate; with additional parameter optimization, this framework will be accessible and implementable for a variety of circuit contexts, enabling researchers more precise and predictable control over the dynamic properties of gene expression.

CHAPTER 2: THE ROLE OF MATHEMATICAL MODELING IN SYSTEMS & SYNTHETIC BIOLOGY – A CASE STUDY

Rationale

Synthetic biology is historically deeply intertwined with the use of mathematical modeling and simulation in the design of novel biological circuits. The works widely recognized as the first two primary articles in synthetic biology are heavily reliant on the use of simple mathematical models to optimize the parameters necessary to achieve the desired functionality, and to predict the outputs of their newly designed circuits. Both investigators utilized systems of ordinary differential equations to evaluate the stability of their circuit's desired behavior under varied conditions (Elowitz & Leibier, 2000; Gardner, Cantor, & Collins, 2000). As the field continues to develop and turns to more complex questions and systems, however, the construction of quantitative models faces exponentially larger challenges: the introduction of dynamical complexity, increase in number of network components and states, and uncertainties in parameterization offer major challenges to constructing a robust and accurate model (Le Novere, 2015). Regardless, a carefully constructed model can play a crucial role in elucidating complex biological mechanisms such as pattern formation, especially when supplemented with quantitative empirical observations.

Here I choose a biological system of interest, the Notch signaling pathway, and delve into the use of mathematical modeling to improve the understanding and control over this system. I will evaluate different iterations of models describing the system and discuss the advantages and limitations of using models to represent this signaling pathway. Notch is a highly conserved signaling pathway which is responsible for a massive variety of cellular behaviors and decisions,

including cell-fate determination and pattern formation during development (Sjöqvist & Andersson, 2019). While within a biological context it has been found that there exist many varieties of Notch ligands, each of which confers complex differences in signal processing and gene expression outcomes (Bray, 2016), for the purposes of this analysis I will focus on the generalizable aspects of Notch behavior and the mathematical modeling thereof; I will then comment on the limitations and potential elaborations upon this approach.

Background & Early Models

The Notch signaling pathway is characterized by juxtacrine interactions between a sender cell, which expresses the membrane-bound Delta ligand, and a receiver cell, which expresses the membrane-bound Notch receptor. The mechanical force of the interaction between Delta and Notch induces regulated intramembrane proteolysis (RIP) within the Notch protein, resulting in a release of the Notch Intracellular Domain (NICD), which is transported to the nucleus to activate target genes (Gordon et al., 2015; Sprinzak et al., 2010). The lack of intermediates between the membrane receptor and the gene expression change in the nucleus means that there is no signal amplification, unlike many other signaling pathways involving phosphorylation cascades and more complex signal transduction. This lack of signal amplification makes the Notch pathway relatively more accessible from a mathematical modeling standpoint (Bray, 2016).

The Notch pathway was first modeled in 1996 by Joanne Collier and colleagues. They formulated a simple system of ordinary differential equations to simulate pattern formation via Notch-mediated lateral inhibition (Collier, Monk, Maini, & Lewis, 1996). This model was later adjusted in 2010 to incorporate the phenomenon of mutual inactivation, where the Delta ligand expressed on a cell interacts with and inhibits the activity of a Notch receptor expressed on the same cell membrane (also knows as *cis*-interaction or *cis*-inhibition) (Sprinzak et al., 2010). We

can simulate this model without any feedback, as a simple mutual inactivation model to describe

boundary formation, or a negative feedback component can be added to describe lateral

inhibition patterning. The mutual inactivation model consists of a set of ordinary differential

equations describing the concentrations of Notch, Delta, and the NICD which produces the

output for the pathway (represented here by S) (Equation 1) (Sprinzak et al., 2010).

On its own, we see that this set of ordinary differential equations produces an

ultrasensitive switch between 2 cell fates: a "sending" state, where the cell primarily expresses

the Delta ligand, and a "receiving" state, where the cell preferentially expresses the Notch

receptor. This phenomenon is a product of the mutual inactivation: when production rates of

Notch and Delta are exactly balanced, *cis*-inactivation cancels the activity of both. However, a

slight surplus of either Notch or Delta production leads to a strong preferential expression of that

component. This ultrasensitivity lends itself to the formation of defined boundaries between cell

types. Notably, this boundary formation is dependent not on the absolute concentrations of Notch

and Delta, but rather the ratio between the two expression levels, making the process robust to

extrinsic noise (Sprinzak, Lakhanpal, LeBon, Garcia-Ojalvo, & Elowitz, 2011; Sprinzak et al.,

2010).

$$\frac{dN}{dt} = \beta_N - \gamma N - \frac{DN}{k_c} - \frac{D_{trans}N}{k_t}$$

$$\frac{dD}{dt} = \beta_D - \gamma D - \frac{DN}{k_c} - \frac{DN_{trans}}{k_t} \qquad (1)$$

$$\frac{dS}{dt} = \frac{DN_{trans}}{k_t} - \gamma_S S$$

Equation 1: Mutual Inactivation model described by Sprinzak and colleagues. N, D are

concentrations of Notch and Delta, respectively. β terms represent production rates; γ terms

represent degradation rates. D_{trans} and N_{trans} represent concentrations of Delta and Notch, respectively, on the neighboring cell with which our cell of interest interacts. k_c and k_t represent the strengths of cis- and trans- interactions, respectively (Sprinzak et al., 2010).

This mutual inactivation model may also be adapted to simulate lateral inhibition patterning, wherein the expression of the Delta ligand is downregulated by the output reporter of Notch activity. Therefore, when a cell receives a signal from a neighboring sender cell, its own Delta production is repressed; this feedback mechanism yields a checkerboard pattern, where a sender cell is surrounded by receiver cells. While other circuit architectures have been proposed to explain lateral inhibition pattern formation via Notch, Sprinzak and colleagues demonstrated that lateral inhibition via mutual inactivation (LIMI) enables robust patterning with a wide range of parameters, and more rapid patterning dynamics than alternative models. Sprinzak also proposes a similar, even simpler circuit architecture involving mutual inactivation, wherein Notch upregulates itself in response to trans-activation (this is called the Simplest Lateral Inhibition with Mutual Inactivation, or SLIMI, circuit). Overall, the superiority of the LIMI and SLIMI models provides a strong rationale for further investigating the role of mutual inactivation *in vivo* during development (Sprinzak et al., 2011).

One foundational Notch behavior which was hypothesized and modeled in detail far more recently is the activation of the Notch receptor by a Delta ligand expressed on the same cell, or cis-activation. Formosa-Jordan and Ibañes produced theoretical predictions via mathematical modeling which posited the possibility of cis-activation, hypothesizing that this form of interaction could act to inhibit pattern formation (Formosa-Jordan & Ibañes, 2014). At the time of that publication, and indeed until recently, there had been no evidence of cis-activation within the Notch pathway in nature (Binshtok & Sprinzak, 2018). However, recent findings from

Nandagopal and colleagues suggest that cis-activation can occur *in vitro* between a variety of ligand and receptor types within the Notch pathway, and within a large variety of cell types. While the influence of this potential interaction *in vivo* remains unclear, it has been hypothesized that *cis*-activation could further expand the possible pattern formation and pattern refinement capabilities of Notch (Nandagopal, Santat, & Elowitz, 2019).

These early models of Notch/Delta interaction provide a strong foundation for the fundamental behaviors of the Notch signaling pathway. Indeed, many of the more recent mathematical models for Notch signaling build directly off of the system of differential equations seen in Equation 1 (Engblom, 2018; Hadjivasiliou, Hunter, & Baum, 2016; Khait et al., 2016; Nandagopal et al., 2019; Shaya et al., 2017; Sprinzak et al., 2011).Using these early models as a starting point, we can now walk through a series of possible additional considerations that may be factored into the mathematical model to more fully address the complexities of *in vivo* signaling. While this is not an exhaustive list, the following models have the advantage of being generalizable and testable within a variety of biological contexts for which Notch plays a key role.

Protrusion-Mediated Signaling

Since the construction of these foundational models, further *in vivo* imaging studies and modeling of bristle pattern formation via lateral inhibition in the *Drosophila melanogaster* notum have revealed that Notch signaling does not exclusively occur between neighboring cells. By comparing the simulations of lateral inhibition based on the early 1996 model with *in vivo* observations of this pattern formation process during bristle precursor differentiation in *Drosophila*, Cohen et al. found that simple lateral inhibition between neighboring cells was not sufficient to explain the spatial distribution of bristle precursor cells. Confocal imaging of the

patterning process revealed the presence of "basal filopodia": transient, actin-based cellular

protrusions which can mediate signaling between non-neighboring cells at an average length of

1.4 cell diameters. To test the hypothesis that these filopodia serve to mediate Notch signaling

between non-neighboring cells, Cohen and colleagues incorporated protrusion-based signaling

dynamics into the mathematical lateral inhibition model. They assumed that signaling was

mediated by filopodia of varying lengths with transient lifetimes. The resulting simulation

revealed a pattern far closer to the observed precursor cell spacing. Using a Neuralized-Gal4,

UAS-Moesin GFP (Neu-GFP) as a marker for Notch activity *in vivo*, Cohen and colleagues

observed GFP-positive basal protrusions mediating cell-cell interactions in the time immediately

prior to cell fate determination, implying that these filopodia may play a role in Notch signaling

during lateral inhibition. They also imaged the same pattern formation process with two different

mutant cell lines in which key regulators of filopodia formation, *scar* and Rac, were knocked

out; these observations revealed irregular spacing compared to wild type pattern formation.

These experiments, in tandem with mathematical modeling, provided strong evidence of

protrusion-mediated Notch signaling during lateral inhibition patterning. (Cohen et al., 2010).

Since this discovery, it has become clear that protrusion-mediated Notch signaling is not limited

to bristle patterning in *Drosophila*—indeed, a similar mechanism was shown to play a role in

zebrafish pigment patterning development (Hamada et al., 2014).

When we move beyond lateral inhibition-based checkerboard patterning, the

phenomenon of protrusion-mediated signaling dramatically diversifies the possible patterns that

can be created via Notch signaling mechanisms (Binshtok & Sprinzak, 2018; Bray, 2016). There

have been several efforts to incorporate protrusion-mediated signaling into mathematical Notch

models to explore the possibilities of this space. In the most recent iteration, Hadjivasiliou and

colleagues build a mathematical model based on the mutual inactivation model discussed previously (Equation 1). In addition to incorporating considerations of protrusion-mediated signaling, this model also develops a novel component motivated by the physical mechanism of Notch function, namely the fact that a mechanical force is required for successful Notch proteolysis (Gordon et al., 2015). This requirement implies the possibility that Notch-Delta interaction in *trans* may occur without actual Notch activation if insufficient mechanical force is present. To account for this possibility, the notation from the original model is adjusted slightly to differentiate between <D$_{in}$>, the amount of incoming *trans*-Delta, and <D$_{out}$>, the amount of *trans*-Delta whose binding results in successful Notch activation and release of the NICD (Equation 2) (Hadjivasiliou et al., 2016).

$$\frac{dN}{dt} = \beta_N - \gamma_N N - \frac{DN}{k_c} - \frac{\langle D_{in} \rangle N}{k_t}$$

$$\frac{dD}{dt} = \beta_D \frac{1}{1+R^m} - \gamma_D D - \frac{DN}{k_c} - \frac{D \langle N_{in} \rangle}{k_t} \qquad (2)$$

$$\frac{dR}{dt} = \beta_R \frac{(\langle D_{out} \rangle N)^S}{k_{RS} + (\langle D_{out} \rangle N)^S} - \gamma_R R$$

Equation 2: Hadjivasiliou, Hunter & Baum's amendment to Sprinzak's 2011 lateral inhibition with mutual inactivation model (note that this is similar to Equation 1, with the addition of Delta repression in response to Notch activation). N, D, R are concentrations of Notch, Delta, and intracellular Notch reporter; k$_{RS}$ is the dissociation constant of the intracellular signal. m and s are cooperativity parameters (Hadjivasiliou et al., 2016; Sprinzak et al., 2011). Remaining notation is consistent with Equation 1.

Protrusion-based signaling is incorporated into the model within the definitions of <D$_{in}$>, <D$_{out}$>, and <N$_{in}$>: each is a weighted combination of the summation of protrusional and

junctional contacts from surrounding cells (Equation 3). The weighting parameters factors allow us to account for potential differences in signaling efficiency between protrusional and junctional contact points. Filopodia were modeled as a function of length and protrusion angle. Simulations revealed that adjustment to these parameters, as well as the weighting parameters, produced a wide variety of possible patterns (Hadjivasiliou et al., 2016). As an additional consideration, Vasilopoulos & Painter constructed a similar model in which they accounted for the theoretical possibility of varying the spatial distribution of Delta along the protrusion. While this amendment to the model would theoretically enhance the potential complexity of pattern formation, Hadjivasiliou and colleagues commented that its feasibility is limited by the precision with which a cell could realistically regulate such ligand distribution along an individual protrusion (Hadjivasiliou et al., 2016; Vasilopoulos & Painter, 2016). Further single-cell imaging work is necessary to determine the constraints of this theory.

$$\langle D_{in} \rangle = w_a \langle D_{in}^a \rangle + w_b \langle D_{in}^b \rangle$$

$$\langle N_{in} \rangle = w_a \langle N_{in}^a \rangle + w_b \langle N_{in}^b \rangle \qquad (3)$$

$$\langle D_{out} \rangle = q_a \langle D_{in}^a \rangle + q_b \langle D_{in}^b \rangle$$

Equation 3: Set of equations for the total amounts of incoming Delta, incoming Notch, and incoming Delta leading to Notch activation, respectively. w_a and w_b are weighting parameters for junctional contacts and protrusion-mediated contacts, respectively (same applies for q_a and q_b). $<D_{in}^a>$ represents the sum of incoming Delta from all cells contributing junctional contact; $<D_{in}^b>$ represents sum of incoming Delta from all cells contributing protrusional contact. Analogous notation applies to the remaining variables (Hadjivasiliou et al., 2016).

Within this self-organizing framework, it is prudent to consider the role of stochasticity in Notch-mediated pattern formation. Cohen and colleagues created an asynchronous cellular automata model to simulate lateral inhibition in a population of cells subject to spatial noise, a result of transient protrusion-mediated signaling, and temporal noise, due to fluctuations in protein expression over time. They concluded that both sources of noise contribute to pattern refinement and rearrangement into "more optimal configurations (dense, ordered fine-grained spots…and aligned stripes)" (Cohen, Baum, & Miodownik, 2011). In another study of stochasticity, Engblom adapted the cellular protrusion-based mathematical model from Hadjivasiliou et al. and performed a stochastic simulation of the associated reactions using Gillespie's direct method (Engblom, 2018; Hadjivasiliou et al., 2016).

Membrane Topology & Cell Morphology

While much remains to be learned about the precise intracellular regulatory mechanisms of Notch and Delta transportation to and localization within the membrane, these considerations, alongside cell-cell contact geometry and overall cell morphology, are of potential importance to Notch-mediated cell fate decisions during development (Bray, 2016). These questions are especially relevant when considering the role and signaling efficiency of protrusion-based Notch/Delta interaction in comparison to junctional contact between directly adjacent cells (Khait et al., 2016).

A recent investigation paired fluorescence microscopy assays with mathematical modeling to investigate the dynamic behavior of Notch and Delta within the membrane, as well as Notch/Delta interaction as a function of contact area between cells. The mathematical model consists of a set of four reaction-diffusion equations (Equation 4) which take into account the following processes: Movement of Notch and Delta into and out of the cell membrane via

exocytosis and endocytosis, lateral diffusion of Notch and Delta across the cell membrane, and

Notch/Delta interactions between two cells at the contact area (Khait et al., 2016).

$$\frac{\partial N}{dt} = D_N \nabla^2 N + k_{exo}^N N_0 - k_{endo}^N N + I_b(r)(k^-[NDl] - k^+ NDl)$$

$$\frac{\partial Dl}{dt} = D_{Dl} \nabla^2 Dl + k_{exo}^{Dl} Dl_0 - k_{endo}^{Dl} Dl + I_b(r)(k^-[NDl] - k^+ NDl)$$

$$\frac{\partial [NDl]}{dt} = I_b(r)(D_{[NDl]} \nabla^2 [NDl] + k^+ NDl - k^-[NDl] - k_S[NDl]) \qquad (4)$$

$$\frac{\partial S}{dt} = I_b(r)k_S \int [NDl]d^2r - \gamma S$$

$$I_b(r) = \begin{cases} 1 \ for \ r \leq b \\ 0 \ elsewhere \end{cases}$$

Equation 4: Reaction-Diffusion equations describing concentrations of Notch (N), Delta (Dl),

Notch-Delta complex ([NDl]), and total signal, concentration of the NICD (S). D is the diffusion

constant of lateral diffusion on the cell membrane; exocytosis of Notch and Delta into the cell

membrane from a large cytoplasmic pool with constant concentrations N_0 and Dl_0 occurs at rate

k_{exo}; endocytosis out of the membrane back into the cytoplasmic pool occurs at rate k_{endo}. k^+ and

k^- represent association and dissociation rates, respectively, for the Notch-Delta complex. This

complex is processed at rate k_S to generate the total signal S. We assume that the contact area

between cells is a disk with diameter b; r is our position of interest on the membrane (Khait et

al., 2016).

Using these reaction-diffusion equations, Khait et al. sought to determine the effects of

ligand diffusion and cell-cell contact area on Notch signaling output. They defined a metric

known as diffusion-length scale, λ, to represent the typical distance traveled by a Delta ligand as

it diffuses along the cell membrane before exiting via endocytosis. It was defined as $\lambda =$

$\sqrt{D/k_{endo}}$, where D is the diffusion coefficient for free Delta and k_{endo} is the rate of Delta

endocytosis out of the membrane. Simulations revealed that within the contact area,

concentrations of free Delta are largely depleted, indicating that free ligand quickly complexes

with *trans*-Notch. While free Notch concentrations also decrease, the effect is much less

dramatic; therefore, the diffusion of the ligand was deemed the limiting metric (Khait et al.,

2016).

An analysis of the effects of contact diameter and diffusion-length scale (λ) on Notch

signaling output revealed two major outcomes: if the cell-cell contact diameter is larger than the

diffusion-length scale, then Notch output is proportional to the contact area. However, if contact

diameter is smaller than the diffusion-length scale, then Notch output is far more dependent on

the diffusion of Delta ligands into the contact area. Importantly, this finding speaks to the

predicted signaling efficiency for junctional signaling between adjacent cells as compared to

protrusion-mediated signaling. When contact is initiated via filopodia, signaling efficiency is

expected to be strongly dependent on the diffusion-length scale of the Delta ligand; signaling is

far more dependent on contact area for junctional signaling (Khait et al., 2016).

Interestingly, fluorescence-imaging-based diffusion assays conducted by Khait and

colleagues revealed highly variable diffusion-length scales for the Delta ligand between cells of

the same type. Based on this finding, it was hypothesized that cells may actively regulate

diffusion-scale lengths of membrane ligands such as Delta in order to control Notch signaling

output. Within filopodia, their analysis of Delta transportation dynamics indicated that Delta may

reach protrusional contacts via active transport; these findings imply that active transport of

Delta in filopodia may be regulated as a contributor to control over Notch signaling (Khait et al.,

2016). Further work is necessary to characterize the transportation of Delta ligands along filopodia to determine whether this proposed regulatory mechanism holds true.

A more recent analysis focused on the junctional contact case, in which contact diameter is greater than diffusion-length scale (Khait et al., 2016). Shaya and colleagues supplemented *in vitro* micropatterning experiments with mathematical modeling to investigate the effect of contact area on Notch signaling efficiency. They adapted the Sprinzak 2011 model in the context of lateral inhibition patterning in order to isolate signaling along each cell-cell boundary. Preliminary *in vitro* experiments revealed that cell-cell contact area can be linearly correlated with Notch signaling output, so within the model they took Notch signaling efficiency along each boundary to be proportional to the length of the boundary. They then simulated lateral inhibition-based pattern formation for an irregular lattice of cells with boundaries of varying lengths. Diffusion was not considered within this model, so ligand concentration was assumed to be constant along all cell boundaries (Shaya et al., 2017).

Simulations of cell populations with the adapted lateral inhibition model revealed that cell size significantly affected the cell's Notch signaling fate: small cells tended to become primarily sender cells, and larger cells tended to become receiver cells. It was hypothesized that this outcome is a result of the level of incoming inhibitory signal for a given cell during fate determination: smaller cells with smaller perimeters receive less Notch signal, which leads to a lower NICD concentration, less repression of the Delta ligand, and therefore a higher overall ligand production rate and a sender cell fate. This differentiation pattern was also observed *in vivo* during hair cell selection in the early developmental stages of the chick inner ear—smaller cell phenotypes appeared to preferentially differentiate into hair cells, while larger cells became supporting cells (Shaya et al., 2017).

Receptor/Ligand Variability and Dynamics

While it was initially postulated that Notch signaling fate determination during processes such as lateral inhibition was primarily driven by stochastic differences in concentrations of Notch and Delta (Cohen et al., 2010; Sprinzak et al., 2010), we now know that this fate determination is a product of ligand expression, which appears to be highly regulated on a spatial and temporal level (Bray, 2016; Khait et al., 2016). One key aspect of Notch signaling that has not yet been discussed within this review is the variability in types of Notch receptors and ligands that exist in nature. Mammals possess four different Notch receptor types and five types of Notch ligands (three in the Delta family and two members of the Serrate ligand family) (LeBon, Lee, Sprinzak, Jafar-Nejad, & Elowitz, 2014). Importantly, different ligands appear to affect Notch signaling output differently in terms of signal strength and duration (Bray, 2016). Furthermore, different combinations of ligand/receptor pairings have been shown to differ in strength of *cis-* and *trans-*interactions; each of these combinations remains to be fully characterized (LeBon et al., 2014).

Further complications are introduced with the consideration that in many vertebrate developmental processes, combinations of multiple receptors and ligands are employed (LeBon et al., 2014). While several case-specific *in vitro* studies investigating particular ligand combinations have shed some light on possible interaction patterns (LeBon et al., 2014; Petrovic et al., 2014), The extent to which the differences in *cis-/trans-*interactions from different receptor/ligand pairings have an impact on overall signaling output and pattern formation is unknown; further investigation is necessary to answer this question (Bray, 2016).

Recent work has also found that in some cases, Notch ligand activity may also be dynamically encoded. In 2018, Nandagopal and colleagues reported that two different Delta

ligands, Dll1 and Dll4, result in two differing temporal Notch activity patterns (pulsatile vs sustained activation) when interacting in *trans* with the Notch1 receptor. In a biological context, this was shown to result in two opposing cell differentiation phenotypes. Much of this work was done using time course fluorescence microscopy of co-cultures of sender and receiver cells, in which the NICD was replaced with a Gal4 transcription factor that targeted a Citrine yellow fluorescent protein. Mathematical modeling was used interpret actual Notch activity based the pulsatile action of the reporter, by taking into account the half-life of the Gal4 transcription factor and the mRNA for the reporter protein; using this model they estimated a Notch activity pulse duration of approximately one hour in response to Dll1 ligand interaction. Computational simulations were also used to determine the effects of changing pulse regularity and frequency on the amplitude and variability of Notch signaling; these simulations were used to confirm the distinctive dynamics of the two ligands (Nandagopal et al., 2018). In the future it may be useful to incorporate these dynamical distinctions into the above foundational models for Notch patterning mechanisms, and to further investigate the role of Notch signaling dynamics among other ligand/receptor pairs *in vivo*.

Limitations & Future Directions

While significant progress has been made over the past 10 years in improving upon foundational models of Notch signaling, it is essential to critically consider the utility of these models; this includes a discussion of the limitations of mathematical modeling in this context. For instance, all of the spatial patterning models discussed here are simulated in two dimensions. While this may be closer to a realistic situation in cases such as epithelial cell patterning, it is clearly not fully representative of a biological tissue environment (Shaya et al., 2017). Another consideration that would be essential in representing a truly realistic tissue environment would

be the potential for interactions between Notch signaling and other signaling pathways. Further characterization of the potential opportunities for and consequences of crosstalk with other signaling pathways is needed (Binshtok & Sprinzak, 2018).

Finally, our understanding of the physical mechanisms surrounding Notch signaling, from transportation of the Notch components within the cell to the physical force necessary for successful Notch activation, is a limitation to providing a realistic, accurately parameterized model. One particular challenge is understanding the specific role of endocytosis in Notch activation and NICD release, on the level of a single Notch/ligand pairing in neighboring cells and protrusions (Hadjivasiliou et al., 2016) as well as clusters of ligand/receptor pairings (Nandagopal et al., 2018). Thus, there is a need to improve upon quantitative measurement and imaging techniques to observe and quantitatively characterize these phenomena *in vivo* and to learn the necessary dynamics and stoichiometries for successful Notch signal processing and pattern development (Bray, 2016).

While these limitations, along with the potential errors associated with parameterization and computational error of order (Engblom, 2018), present a challenge to the utility of mathematical modeling of Notch signaling, the above examples demonstrate that an interplay between mathematical modeling and empirical testing enables researchers to gain new understanding of these complex biological processes. These mathematical models are certainly not precise representations of the associated biological events; however, these simulations provide a useful framework by which one can generate testable hypotheses and predict potential outcomes without costly biological experimentation (Binshtok & Sprinzak, 2018). Therefore, the use and continuous improvement of mathematical models to represent complex biological

processes such as Notch signaling is essential for efficient and thorough investigation of these phenomena.

CHAPTER 3: CONTRIBUTIONS TO A SYNTHETIC BIOLOGY INFRASTRUCTURE AT WILLIAM & MARY

Current Status

Despite the lack of a Bioengineering Department or Engineering School, or even faculty specializing in the field of synthetic biology, the College of William & Mary has garnered available resources and significantly enhanced a research program and research opportunities for undergraduates in the field of synthetic biology over the past five years. The introduction of new coursework, a dedicated Bioengineering Lab space, and independent and team-based research opportunities are the first steps in building a platform for undergraduate students to be introduced to synthetic biology. There are still many opportunities to continue to increase the resources and accessibility for undergraduate students to empower them to engage in original research projects at the cutting edge of the field. However, the current resources and opportunities for students create a solid foundation upon which additional avenues for research can be built.

On an academic level, students are presented with two major opportunities to engage with synthetic biology: The Freshman Honors Biology lab, and the one-credit Readings in Synthetic Biology seminar. Open to all students, this seminar has primarily been led by undergraduate teaching assistants. It takes on a journal club format, where students take turns leading discussions on recently published primary articles. This course has, in part, served as a primer for students interested in joining the William & Mary iGEM team, whose contribution to synthetic biology at William & Mary will be discussed below. However, even apart from iGEM, it also

provides a solid theoretical framework for students who in many cases have little to no experience with synthetic biology, allowing them to improve their primary literature analysis skills and gain an understanding of the current state of the field.

The Freshman Honors Biology lab is available to students entering William & Mary who have earned a score of 5 on the AP Biology exam. It offers an opportunity for these students to opt out of the introductory biology lab class and jump straight into building their research skills, incorporating elements of primary literature analysis and molecular biology lab techniques along a theme of synthetic biology. Finally, students are encouraged to apply the techniques they learned by engaging in self-directed research. In the most recent semester the course was offered, freshman students had the opportunity to choose between constructing a 3D cell printer from scratch or learning about mammalian cell culture techniques and the potential research avenues within mammalian synthetic biology. Importantly, both this course and the Readings seminar course are led by undergraduate student teaching assistants, offering an opportunity not only for students to learn technical skills but for teaching assistants to improve their leadership and communication skills.

Synthetic biology opportunities can be found in not only the coursework at William & Mary, but also in the resources and facilities available to students. The Bioengineering Lab (BEL) was established in the new Integrated Science Center (ISC) wing in 2016 to serve as an interdisciplinary space dedicated to undergraduate research in synthetic biology and other related fields. Since then, the BEL has come to house the William & Mary iGEM team and the Freshman Honors Biology Lab, as well as a workspace for a postdoctoral student from the Cotton lab and 3D printers used by the Sanderson Lab. The equipment available in this lab, as well as in the ISC core lab, have been integral to the work done in this space thus far but present

a tremendous opportunity for use in research focuses that have yet to be explored at William & Mary such as mammalian synthetic biology.

The main driver of undergraduate synthetic biology research at William & Mary has been the International Genetically Engineered Machine (iGEM) team, which has existed at the College since 2014. iGEM is an international synthetic biology competition in which students at the high school, undergraduate, and graduate levels spend the summer creating an original research project. Historically, the W&M iGEM team has focused on foundational work in gene expression measurement and control using *Escherichia coli (E. coli)* as a model organism, to great success on the international level. Notably, iGEM students at W&M have made an effort to expand their work beyond the limited timeline of the competition, communicating their findings at national conferences and by publishing in peer-reviewed journals (Clifton et al., 2018). The evolution of iGEM projects into long-term independent and team projects has contributed to a larger infrastructure for synthetic biology at W&M. Over the years, students have developed a collection of reliable protocols for bacterial cloning techniques, and a wealth of institutional knowledge in both synthetic biology background and troubleshooting techniques. This knowledge and material is passed from senior students to new iGEM members, allowing for a self-sufficient and largely student-driven collective of synthetic biology researchers at W&M.

While the infrastructure for bacterial synthetic biology is steadily growing, there has been relatively little progress in tapping into the quickly growing field of mammalian synthetic biology. This represents a tremendous opportunity for future students to genuinely engage with the cutting edge of what is possible in synthetic biology, whether it be through iGEM or as an independent or team project. Given the existing laboratory spaces and resources, and the strength of student interest in synthetic biology (as demonstrated by high iGEM application rates and

consistent student enrollment in the synthetic biology-related courses), there is an opening for the expansion of undergraduate synthetic biology research at William & Mary to include work within mammalian systems. There exists a major opportunity to jumpstart a sustainable infrastructure for research in mammalian synthetic biology within the Bioengineering Lab, creating an accessible avenue for future students to engage with and make genuine contributions to this exciting field.

A Sustainable Platform for Mammalian Synthetic Biology at W&M

Having served as a participant and as a leader or formal teaching assistant in all of the synthetic biology initiatives mentioned above over the past four years at William & Mary, the aim of this project was to leave a lasting impact by creating a sustainable infrastructure through which students can pursue self-driven research in mammalian synthetic biology in years to come. By building off the existing resources and infrastructure, we have created a space for work in mammalian tissue culture. This was accomplished via a multifaceted approach: by working to build up student awareness of and interest in the exciting field of synthetic biology, designing a dedicated workspace for mammalian tissue culture in the Bioengineering Lab, creating new opportunities for student-directed research and independent study in this space, and creating written standardized protocols so that students may quickly learn the necessary techniques to rigorously execute a research project with mammalian cells. Moving forward, students will be able to build off this foundation to delve into the cutting edge of mammalian synthetic biology, incorporating the use of existing resources at W&M such as the Fluorescence Activated Cell Sorter (FACS) and the fluorescence microscope in the BEL to gather high quality data.

Essential to building a foundation for mammalian synthetic biology is raising student awareness of and interest in the field. To that end, I led the spring semester for the Readings in

Synthetic Biology seminar course. This course was led in the style of a journal club, with a focus on current research (primarily from the past 3 years). After a brief introduction to the field as a whole, students took turns choosing and leading discussions on primary articles based on their own interests. Discussions focused heavily on motivations, methodology, and future directions, encouraging students to approach the articles critically and reflect on the big-picture impacts of the work. Students were allowed to choose an article based on their own interests in addition to leading the discussions; thus, they were challenged to not only gain a thorough understanding of their article of choice but to spend time exploring the diversity of possible research questions and applications within the field. Since the majority of students in this seminar are underclassmen, the aim of this seminar structure was to garner interest and excitement about the massive potential of synthetic biology research.

While the main Bioengineering Lab is currently home to the iGEM team, and also utilized by Dr. Sanderson and Dr. Cotten, there is a prep room off of the main lab which houses the biological safety cabinet, CO_2 incubator, and fluorescence microscope. With the assistance and resources provided by the university, this room was adapted into a fully stocked tissue culture room which could be used for mammalian cell culturing and experimentation. The room was re-organized, the incubator was cleaned and calibrated, and the space was stocked with all of the materials required for tissue culture work, including a vacuum-powered aspirating system. While much of the school year was spent setting up the lab space and researching and ordering the necessary materials, I have also begun to mentor and train three freshman students in tissue culture techniques. These students have all expressed serious interest in continuing with mammalian synthetic biology work in the coming year. Together, we have begun culturing a CHO-K1 cell line in order to learn and practice aseptic technique, feeding, and passaging cells.

Beyond the setup of the lab itself, it is essential that a strong foundation of background knowledge exists so that lab work can continue seamlessly despite student turnover. Over the years, the iGEM team has established a thorough set of standardized protcols for bacterial cloning techniques. This year we wrote an additional set of protocols for common techniques in mammalian cell culture compiled from protocol recommendations from established institutions such as Rice University and providers such as ATCC and Invitrogen (Atcc, 2014; Atcc, Invitrogen, & Dopico, 2014).These protocols, stored on the online lab notebook software Benchling, include Thawing Cells, Feeding Cells, Subculturing and Transfection (full protocols can be found in Appendix III). We have also included guidelines for aseptic technique, set up and clean up for cell culture work, and compiled a Beginner's Guide to Mammalian Cell Culture as an accessible guide for those completely new to the lab environment (these can also be found in Appendix III). These protocols and guidelines could potentially be incorporated into the curriculum for future semesters of the Freshman Honors Biology Lab, so that freshmen interested in research are introduced to the option of cell culture work in the context of synthetic biology.

In the coming months, after we are fully comfortable with working with the cells and have determined appropriate split ratios, our next step will be to attempt a simple GFP transfection. This will allow us to not only practice a new technique, but also to practice the use of the fluorescence activated cell sorter (FACS) and fluorescence microscope, the use of which will be essential to data collection for more complex projects. One of my mentees has elected to remain at William & Mary in the summer to continue working in the cell culture lab in the BEL. Ultimately, she aims to design a research project focusing on the Notch pathway, which will be

made possible given the resources available at W&M and the infrastructure that has been established.

Moving forward, this project will ensure that mammalian synthetic biology is incorporated and maintained as an integral component of the synthetic biology and bioengineering research at William & Mary. There exists a group of students who are strongly interested in continuing mammalian synthetic biology research in the coming years, and the Readings in Synthetic Biology course will continue to urge students to consider pursuing research in synthetic biology, whether it be through iGEM, with the mammalian cell culture team, or as part of an independent project in the BEL. We hope to coordinate with W&M iGEM team members over the summer and encourage them to consider working with mammalian cells as a possible aspect of their iGEM project, or alternatively to workshop with them to introduce them to mammalian cell culture techniques so that they may be incorporated into future projects. Ultimately, it is our goal to create an established, accessible and sustainable foundation for mammalian synthetic biology such that students will be able to not only learn about and explore this exciting field but also to make genuine contributions to the field in the form of peer-reviewed publications in the years to come.

References

Alon, U. (2006). *An Introduction to Systems Biology: Design Principles of Biological Circuits* (1st ed.). Chapman and Hall/CRC.

Anderson, J. C., Voigt, C. A., & Arkin, A. P. (2007). Environmental signal integration by a modular and gate. *Molecular Systems Biology*. https://doi.org/10.1038/msb4100173

Atcc. (2014). Animal Cell Culture Guide. *Atcc*. https://doi.org/10.1093/chemse/bjt099

Atcc, Invitrogen, & Dopico, A. (2014). Cell Culture Basics Handbook. *Atcc*. https://doi.org/10.1093/chemse/bjt099

Binshtok, U., & Sprinzak, D. (2018). Modeling the notch response. In *Advances in Experimental*

Medicine and Biology. https://doi.org/10.1007/978-3-319-89512-3_5

Bray, S. J. (2016). Notch signalling in context. *Nature Reviews Molecular Cell Biology*. https://doi.org/10.1038/nrm.2016.94

Cameron, D. E., & Collins, J. J. (2014). Tunable protein degradation in bacteria. *Nature Biotechnology*. https://doi.org/10.1038/nbt.3053

Castillo-Hair, S. M., Sexton, J. T., Landry, B. P., Olson, E. J., Igoshin, O. A., & Tabor, J. J. (2016). FlowCal: A User-Friendly, Open Source Software Tool for Automatically Converting Flow Cytometry Data from Arbitrary to Calibrated Units. *ACS Synthetic Biology*. https://doi.org/10.1021/acssynbio.5b00284

Clifton, K. P., Jones, E. M., Paudel, S., Marken, J. P., Monette, C. E., Halleran, A. D., … Saha, M. S. (2018). The genetic insulator RiboJ increases expression of insulated genes 06 Biological Sciences 0604 Genetics. *Journal of Biological Engineering*, *12*(1). https://doi.org/10.1186/s13036-018-0115-6

Cohen, M., Baum, B., & Miodownik, M. (2011). The importance of structured noise in the generation of self-organizing tissue patterns through contact-mediated cell-cell signalling. *Journal of the Royal Society Interface*. https://doi.org/10.1098/rsif.2010.0488

Cohen, M., Georgiou, M., Stevenson, N. L., Miodownik, M., & Baum, B. (2010). Dynamic Filopodia Transmit Intermittent Delta-Notch Signaling to Drive Pattern Refinement during Lateral Inhibition. *Developmental Cell*. https://doi.org/10.1016/j.devcel.2010.06.006

Collier, J. R., Monk, N. A. M., Maini, P. K., & Lewis, J. H. (1996). Pattern formation by lateral inhibition with feedback: A mathematical model of delta-notch intercellular signalling. *Journal of Theoretical Biology*. https://doi.org/10.1006/jtbi.1996.0233

Elowitz, M. B., & Leibier, S. (2000). A synthetic oscillatory network of transcriptional regulators. *Nature*. https://doi.org/10.1038/35002125

Engblom, S. (2018). Stochastic Simulation of Pattern Formation in Growing Tissue: A Multilevel Approach. *Bulletin of Mathematical Biology*. https://doi.org/10.1007/s11538-018-0454-y

Formosa-Jordan, P., & Ibañes, M. (2014). Competition in notch signaling with cis enriches cell fate decisions. *PLoS ONE*. https://doi.org/10.1371/journal.pone.0095744

Gardner, T. S., Cantor, C. R., & Collins, J. J. (2000). Construction of a genetic toggle switch in Escherichia coli. *Nature*. https://doi.org/10.1038/35002131

Gordley, R. M., Williams, R. E., Bashor, C. J., Toettcher, J. E., Yan, S., & Lim, W. A. (2016). Engineering dynamical control of cell fate switching using synthetic phospho-regulons. *Proceedings of the National Academy of Sciences*. https://doi.org/10.1073/pnas.1610973113

Gordon, W. R., Zimmerman, B., He, L., Miles, L. J., Huang, J., Tiyanont, K., … Blacklow, S. C. (2015). Mechanical Allostery: Evidence for a Force Requirement in the Proteolytic Activation of Notch. *Developmental Cell*. https://doi.org/10.1016/j.devcel.2015.05.004

Gur, E., & Sauer, R. T. (2008). Evolution of the ssrA degradation tag in Mycoplasma: Specificity

switch to a different protease. *Proceedings of the National Academy of Sciences*. https://doi.org/10.1073/pnas.0808802105

Hadjivasiliou, Z., Hunter, G. L., & Baum, B. (2016). A new mechanism for spatial pattern formation via lateral and protrusionmediated lateral signalling. *Journal of the Royal Society Interface*. https://doi.org/10.1098/rsif.2016.0484

Hamada, H., Watanabe, M., Lau, H. E., Nishida, T., Hasegawa, T., Parichy, D. M., & Kondo, S. (2014). Involvement of Delta/Notch signaling in zebrafish adult pigment stripe patterning. *Development*. https://doi.org/10.1242/dev.108894

Jones, E. M., Monette, C. E., Marken, J. P., Dhawan, S., Gibney, T., Li, C., … Saha, M. (2018). Modular, part-based control of gene expression response time using protein degradation tags. *BioRxiv*, 482331. https://doi.org/10.1101/482331

Kelly, J. R., Rubin, A. J., Davis, J. H., Ajo-Franklin, C. M., Cumbers, J., Czar, M. J., … Endy, D. (2009). Measuring the activity of BioBrick promoters using an in vivo reference standard. *Journal of Biological Engineering*. https://doi.org/10.1186/1754-1611-3-4

Khait, I., Orsher, Y., Golan, O., Binshtok, U., Gordon-Bar, N., Amir-Zilberstein, L., & Sprinzak, D. (2016). Quantitative Analysis of Delta-like 1 Membrane Dynamics Elucidates the Role of Contact Geometry on Notch Signaling. *Cell Reports*. https://doi.org/10.1016/j.celrep.2015.12.040

Le Novere, N. (2015). Quantitative and logic modelling of molecular and gene networks. *Nature Reviews Genetics*. https://doi.org/10.1038/nrg3885

LeBon, L., Lee, T. V, Sprinzak, D., Jafar-Nejad, H., & Elowitz, M. B. (2014). Fringe proteins modulate Notch-ligand cis and trans interactions to specify signaling states. *ELife*. https://doi.org/10.7554/elife.02950

Maeda, Y. T., & Sano, M. (2006). Regulatory Dynamics of Synthetic Gene Networks with Positive Feedback. *Journal of Molecular Biology*. https://doi.org/10.1016/j.jmb.2006.03.064

Nandagopal, N., Santat, L. A., & Elowitz, M. B. (2019). Cis-activation in the Notch signaling pathway. *ELife*. https://doi.org/10.7554/elife.37880

Nandagopal, N., Santat, L. A., LeBon, L., Sprinzak, D., Bronner, M. E., & Elowitz, M. B. (2018). Dynamic Ligand Discrimination in the Notch Signaling Pathway. *Cell*. https://doi.org/10.1016/j.cell.2018.01.002

Nielsen, A. A. K., Der, B. S., Shin, J., Vaidyanathan, P., Paralanov, V., Strychalski, E. A., … Voigt, C. A. (2016). Genetic circuit design automation. *Science*. https://doi.org/10.1126/science.aac7341

Petrovic, J., Formosa-Jordan, P., Luna-Escalante, J. C., Abello, G., Ibanes, M., Neves, J., & Giraldez, F. (2014). Ligand-dependent Notch signaling strength orchestrates lateral induction and lateral inhibition in the developing inner ear. *Development*. https://doi.org/10.1242/dev.108100

Rosenfeld, N., Elowitz, M. B., & Alon, U. (2002). Negative autoregulation speeds the response times of transcription networks. *Journal of Molecular Biology*.

https://doi.org/10.1016/S0022-2836(02)00994-4

Shaya, O., Binshtok, U., Hersch, M., Rivkin, D., Weinreb, S., Amir-Zilberstein, L., … Sprinzak, D. (2017). Cell-Cell Contact Area Affects Notch Signaling and Notch-Dependent Patterning. *Developmental Cell*. https://doi.org/10.1016/j.devcel.2017.02.009

Siuti, P., Yazbek, J., & Lu, T. K. (2013). Synthetic circuits integrating logic and memory in living cells. *Nature Biotechnology*. https://doi.org/10.1038/nbt.2510

Sjöqvist, M., & Andersson, E. R. (2019). Do as I say, Not(ch) as I do: Lateral control of cell fate. *Developmental Biology*. https://doi.org/10.1016/j.ydbio.2017.09.032

Sprinzak, D., Lakhanpal, A., LeBon, L., Garcia-Ojalvo, J., & Elowitz, M. B. (2011). Mutual inactivation of Notch receptors and ligands facilitates developmental patterning. *PLoS Computational Biology*. https://doi.org/10.1371/journal.pcbi.1002069

Sprinzak, D., Lakhanpal, A., Lebon, L., Santat, L. A., Fontes, M. E., Anderson, G. A., … Elowitz, M. B. (2010). Cis-interactions between Notch and Delta generate mutually exclusive signalling states. *Nature*. https://doi.org/10.1038/nature08959

Vasilopoulos, G., & Painter, K. J. (2016). Pattern formation in discrete cell tissues under long range filopodia-based direct cell to cell contact. *Mathematical Biosciences*. https://doi.org/10.1016/j.mbs.2015.12.008

Appendix I: Experimental Methods for Degradation-Based Control of Gene Expression Response Time

Construct Design & Assembly

Sequences for pdts and mf-Lon were provided by the Cameron & Collins 2014 article (Cameron & Collins, 2014); these sequences were codon-optimized for *E. coli* and synthesized as gene blocks. ATc-inducible reporter constructs were cloned using Gibson Assembly to create the following part sequence: pTet promoter – B0034 RBS - mScarlet-I – pdt – B0015 terminator followed by a constitutively expressed TetR repressor whose repression of the pTet promoter is relieved by ATc. This sequence of parts was cloned onto the pSB1C3 chloramphenicol-resistant high-copy plasmid backbone. Likewise, the mf-Lon sequence was placed under the control of the IPTG-inducible pLac0-1 promoter using Gibson assembly; on the same plasmid, we added a

constitutively expressed LacI repressor whose repression of the pLac0-1 promoter is relieved by the outside addition of IPTG. This protease construct was added to the medium-copy backbone pSB3K3, which includes kanamycin resistance gene.

Circuit Response Time Characterization

ATc-inducible reporter constructs were co-transformed with the IPTG-inducible protease construct into the 10-Beta strain of *E. coli*. Colonies were grown on chlor + kan agar plates and inoculated into M9 minimal media with 0.4% glycerol overnight. The following day, cultures were diluted 1:100 into fresh M9 media and allowed to grow for an additional 4-7 hours, then diluted once more to an optical density (OD) of 0.01 into M9 media containing 0.1mM IPTG and 50ng/mL ATc to begin the time course experiment. Time points were taken every 20 minutes onto ice and immediately measured using flow cytometry (at least 10,000 single cell measurements). The FACS was calibrated by taking 10,000 measurements of Rainbow Calibration Particles from Spherotek on each day when measurement occurred. These measurements were used along with the python package flowcal (Castillo-Hair et al., 2016) to convert sample fluorescenct to units of Molecules of Equivalent FLuorescein (MEFLs).

This account of experimental methods has been adapted from Jones, Monette, et al. (Jones et al., 2018).

Author Contributions

Constructs and experiments were designed by Ethan Jones with assistance from Callan Monette. Constructs were cloned and experiments carried out by Callan Monette and Ethan Jones, with assistance from Sejal Dhawan, Theresa Gibney, Christine Li, Alyssa Luz-Ricca, and Cici Zheng. Ethan Jones, John Marken, Wukun Liu, and Cedar Ren analyzed data, John Marken and Ethan

Jones produced the figures. All of the above participants helped conceive the project. This work is published as a pre-print on BioRxiv; the manuscript was written with equal contributions by Callan Monette and Ethan Jones (Jones et al., 2018).

Appendix II: Readjustment of Protein Steady-State Concentration

A notable consideration when manipulating protein degradation rate to decrease gene expression response time is the resulting decrease in the resulting output steady state due to degradation of the product (Figure i). This outcome may be problematic in the context of a more complex gene network, where there may be a need to speed up the output of a given node while maintaining said output above a desired threshold of expression magnitude. Fortunately, given that our model dictates that the steady state output for an inducible gene is equal to α/γ and that our expression response time can be controlled by changing degradation alone, we expect that increasing production rate will independently increase the output steady state without affecting response time outcome.
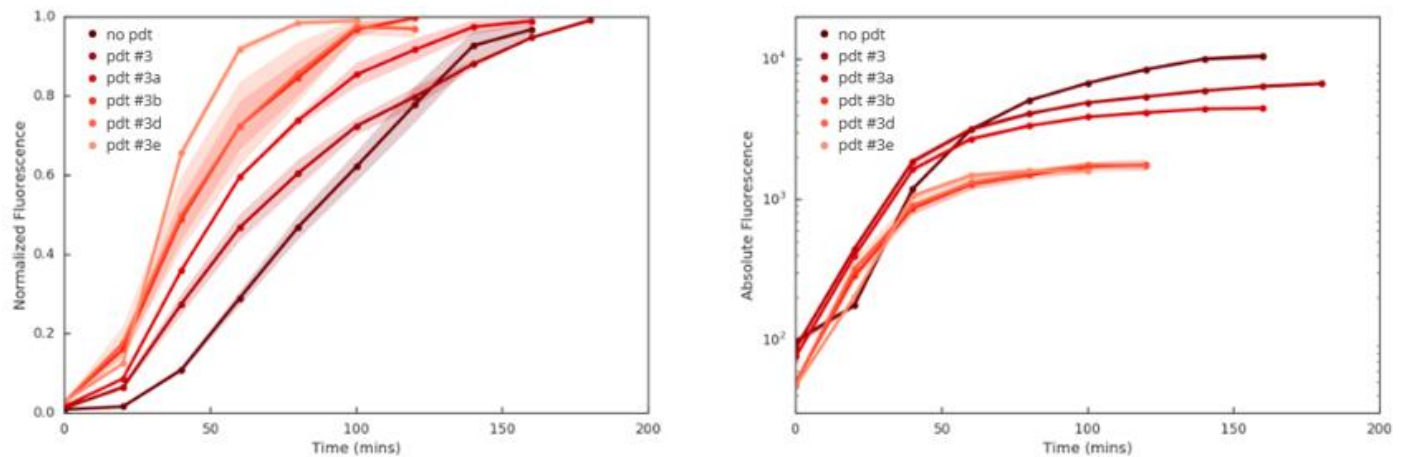

Figure i: *(Left) Normalized and (Right) Absolute fluorescence measurements for reporter expression response time over the course of 200 min. Absolute fluorescence time course*

illustrates the decrease in steady state output due to the higher degradation rates for constructs

tagged with pdts of higher protease affinity.

As a proof-of-concept, we demonstrated that steady state readjustment could be achieved by increasing the ATc inducer concentration for one of our inducible tagged reporter constructs. As predicted by the model, we successfully demonstrated that production rate could be manipulated independently from the response time change conferred by a change in degradation rate (Figure ii).
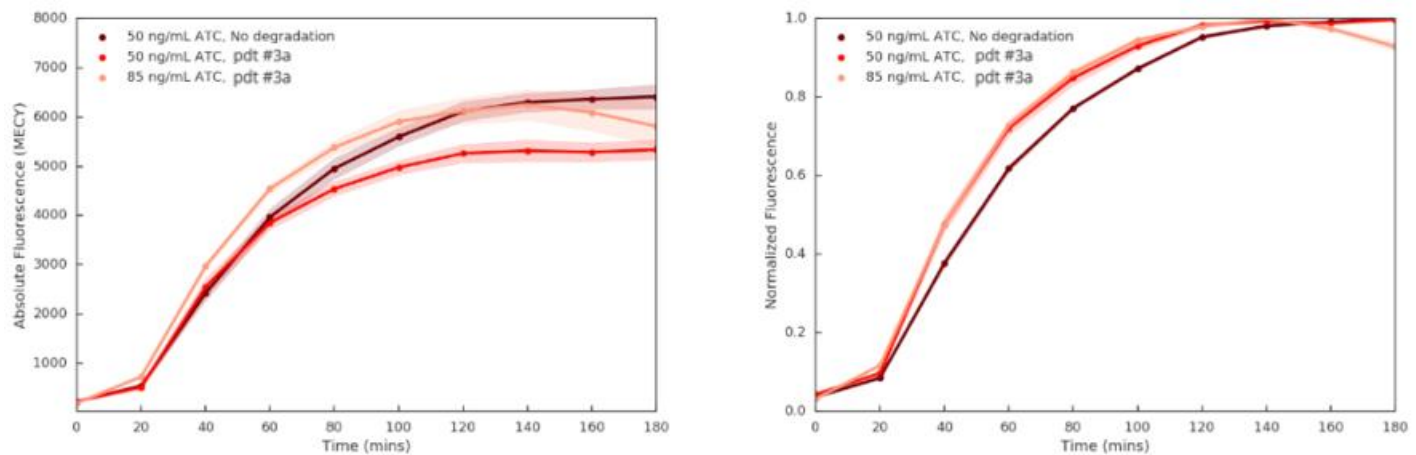

Figure ii: (Left) Absolute fluorescence time course demonstrating the decrease in steady state with the addition of pdt#3a; this change was readjusted with the increase of inducer concentration from 50ng/mL to 85ng/mL ATc, to achieve a steady state similar to that of the tagless control. (Right) A normalized version of the same time course demonstrates that the change in response time remains consistent between the lower and higher induction conditions, implying that production rate can be manipulated independently from response time control via degradation.

Appendix III: Mammalian Cell Culture Protocols and Guidelines

Beginner's Guide to Mammalian Cell Culture

THURSDAY, 4/18/2019

Welcome to the BEL's Mammalian Synthetic Biology lab! Before you get started, there are a number of basic concepts and techniques that you will need to learn.

BACKGROUND READING

To begin, if you are completely new to the field of synthetic biology, or would like to brush up on a history and overview of the field, this guide provides a useful summary of how the field began and where it is headed next:

📎 Davies_SynBioIntro_PartI.pdf

📎 Davies-SynBioIntro_Part2.pdf

Next, we will focus in on the topics and challenges releavant to performing synthetic biology within mammalian systems:

📎 Black_MammSynBio_AnnRev-2017.pdf

📎 Mathur_MammalianCellBioForStudyingCell_2017.pdf

LAB TECHNIQUES

As a general reference and guide to cell culture, ATCC and Invitrogen both have comprehensive guides to cell culture lab technique. No need to read these cover to cover, but they are very useful if you would like to learn more about a particular protocol or trying to troubleshoot a problem.

Invitrogen: https://www.vanderbilt.edu/viibre/CellCultureBasicsEU.pdf
(https://www.vanderbilt.edu/viibre/CellCultureBasicsEU.pdf)
ATCC: https://www.atcc.org/~/media/pdfs/culture%20guides/animcellculture_guide.ashx
(https://www.atcc.org/~/media/pdfs/culture%20guides/animcellculture_guide.ashx)

The linked videos are taken from Rice University's Bioengineering Tissue Culture Lab course. While their lab setup and media may be slightly different than what we will use, these videos provide a useful explanation of sterile techniques, and relevant advice for improving cell viability during subculturing etc.

Lab Setup/Cleanup, Equipment and Aseptic Technique:
Lab Set Up: https://www.youtube.com/watch?v=EOxEFFcj21g (https://www.youtube.com/watch?v=EOxEFFcj21g)
Hood (Part 1): https://www.youtube.com/watch?v=AZ0fhvtX7vE&feature=youtu.be (https://www.youtube.com/watch?v=AZ0fhvtX7vE&feature=youtu.be)
Hood (Part 2): https://www.youtube.com/watch?v=ZG9QOnqMYNU&feature=youtu.be (https://www.youtube.com/watch?v=ZG9QOnqMYNU&feature=youtu.be)
Pipette: https://www.youtube.com/watch?v=HuuXdZEv-UU&feature=youtu.be (https://www.youtube.com/watch?v=HuuXdZEv-UU&feature=youtu.be)

BEL-specific protocols:

📄 Aseptic Technique Guidelines

📄 Cleanup Checklist

Essential Protocols:

📱 Feeding Cells

📱 Subculturing / Passaging Cells

Cell Passage (Part 1): https://www.youtube.com/watch?v=_TkGgk4xies&feature=youtu.be (https://www.youtube.com/watch?v=_TkGgk4xies&feature=youtu.be)

Cell Passage (Part 2): https://www.youtube.com/watch?v=Ic7Kig9WyQs&feature=youtu.be (https://www.youtube.com/watch?v=Ic7Kig9WyQs&feature=youtu.be)

Cell Passage (Part 3): https://www.youtube.com/watch?v=AxgwbqGwgYc&feature=youtu.be (https://www.youtube.com/watch?v=AxgwbqGwgYc&feature=youtu.be)

Split Ratio: https://www.youtube.com/watch?v=KTfazqvTweU&feature=youtu.be (https://www.youtube.com/watch?v=KTfazqvTweU&feature=youtu.be)

Aseptic Technique Guidelines

SUNDAY, 4/7/2019

Outside of the hood:

- Adhere to BSL1 Safety Guidelines: Avoid open toed shoes and shorts, tie back long hair, no food or water allowed in lab. Do not apply chapstick or cosmetics in lab.
- Wear gloves at all times when handling cells/reagents. Spray gloved hands with ethanol.
- Avoid touching face, hair, phone/computer, etc. while wearing gloves
- Before beginning work, wipe down work area with 70% ethanol
- Avoid talking, singing, or whistling while working in the TC room

Handling reagents:

- Aliquot all reagents. Avoid pipetting straight from stock solution
- Never pour liquid back into the stock container
- Carefully inspect reagents before use. If liquid appears cloudy, discolored, or otherwise contaminated, discard and use a fresh aliquot.
- Avoid pouring media/reagents directly from bottles/flasks
- Ensure all containers are tightly sealed at all times when not in use

In the hood:

- Close the hood when you are not actively working in it; when in use, minimize the amount it is open
- Keep hood neat and work area clear
- Ensure necessary materials (pipettes, flasks, falcon tubes) are in the hood before you begin working
- Most sterile parts of the hood are middle/back
  - Trash and other materials not in use should be stored along the outside edges of the hood
- Disinfect work area with ethanol before and after procedures, and if any spillage occurs
- Sterilize ALL ITEMS with 70% ethanol before bringing them into the hood
  - For electronic pipettor/other sensitive items, wipe with an ethanol-soaked kimwipe or paper towel
- Keep arms/elbows off of work surface
- Leave bottles/flasks covered as much as possible--do not remove cap until the moment you need to, replace cap as soon as possible
- If you remove a cap or cover, and have to put it down on the work surface, place the cap at the back of the hood with opening facing down
- Avoid opening multiple bottles/tubes at the same time if possible
- Do not unwrap pipettes until they are ready to be used; use each pipette only once

Preparing Media for CHO-K1 Cells

Introduction

For CHO-K1 cells (ATCC CCL-61), the base medium for this cell line is ATCC-formulated F-12K Medium. To make the complete growth medium, add the following components to the base medium: fetal bovine serum to a final concentration of 10%. Prepare the following in the laminar flow hood to prevent contamination.

Note: F-12K medium should be stored in the dark when not in use at 2-8C. If stored in the refrigerator, wrap in aluminum foil.

Materials

› ATCC-formulated F-12K Medium

› Fetal Bovine Serum

› Falcon Tubes (15 mL or 50 mL)

Procedure

Aliquot FBS for long-term storage

1. Aliquot 15 mL of FBS into Falcon Tubes

2. Store in -20C for long-term storage, 500 mL bottles are stored in the -80C

Create 50 mL aliquots of supplemented media

3. Aliquot 45 mL of media into falcon tubes (labelled w/date)

4. To the F-12K media, add:

   5 mL FBS, to 10% volume
   If desired, antibiotic to 1% volume

5. Store in +4ºC in TC room (can be stored in the fridge for up to 6 months)

Thawing Frozen Cells

Introduction

Mammalian cells are shipped and preserved using dry ice/liquid nitrogen. Here we describe how to thaw cells that have been stored or recently purchased to start a new line. NOTE: Be sure to check the requirements (media/supplement type, centrifugation parameters) of the specific cell type you are working with before beginning.

As with all cell cutlure techniques, be sure to pay special attention to sterile technique--spray your hands and all materials with ethanol before they enter the laminar flow hood, tighten all caps before they leave the hood.

Materials

> Water bath, warmed to 37C

> Cryovial with frozen cells

> Appropriate supplemented media

> Culture vessel (T25 or T75 tissue culture-grade flask)

> Centrifuge tube (15mL Falcon tube)

> Pipettes (10mL, 2mL)

Procedure

Preparation

1. Pre-warm appropriate culture medium in water bath to 37C

2. Set out necessary pipettes/other materials next to the hood before beginning

3. Prepare a culture vessel with the recommended volume of culture medium (depends on cell type); store in incubator until resuspension step

   For a T25 flask, use 5mL
   For a T75 flask, use 10mL

4. Add 9mL warmed media to a centrifuge tube in the laminar flow hood

Thaw Cells

5. Quickly transfer cryovial from liquid nitrogen/dry ice to the 37C water bath. Gently agitate/swirl the tube in the water bath for 1-2 minutes, until the ice crystals have melted.

   Recommended: Relieve the pressure created by rapid temperature change by wetting a kimwipe with 70% ethanol and using this to quickly loosen and re-tighten the cap of the cryovial.

6. Sterilize the cryovial with 70% ethanol and transfer to the laminar flow hood.

7. Carefully transfer the contents of the cryovial dropwise into the centrifuge tube prepared in step 4; screw on cap tightly

Prepare for culturing

8. In a balanced centrifuge, gently spin down cells (ATCC recommends 10 minutes at 125 x g; check requirements of your specific cell type). Spray tube with ethanol and bring it back into laminar flow hood.

9. CAREFULLY aspirate supernatant without disturbing the pellet

10. Gently resuspend cells in 1-2mL pre-warmed complete growth medium by pipetting up and down 15-20 times

11. Transfer resuspended cells to the culture vessel you prepared in step 2; deposit cells into the center of the rectangular base of the flask. Rock flask gently back and forth to distribute the cells evenly.

12. Check for presence of cells using inverted microscope. Store vessel in incubator; examine cell cultures again after 24 hours.

13. It is recommended to replenish with fresh media ~24 hrs after thawing cells.

14. TIP FROM SIGMA ALDRICH: For most cultures it is best practice to subculture before confluence is reached so that the cells are harvested during their log phase of growth and are at optimum viability ready for seeding into new flasks. Furthermore, there are some specific cell types that must be subcultured before confluence is reached in order to maintain their characteristics e.g. the contact inhibition of NIH3T3 cells is lost if they are allowed to reach confluence repeatedly.

Feeding Cells

Introduction

This protocol describes how to replenish the media in your cells. You should replace your cell culture media every 2-3 days to ensure that your cells have the resources they need to survive.

Materials

› Appropriate supplemented media

› T-Flask with growing cell culture

› Aspirating pipette

› 10mL pipette

Procedure

Prepare media

1. Obtain an aliquot of appropriate supplemented media, prewarm at 37C

   Double check whether media is supplemented with 5% or 10% FBS

2. Ensure that the correct pipettes are readily available in the hood

Feed cells

3. Remove the T-flask with cell culture from the incubator, being sure not to touch the culture liquid to the filter on the cap

4. Sterilize the flask (again, avoid spraying ethanol on the filter) and bring it into the hood.

5. Loosen the cap of the T Flask and attach the aspirating pipette to the vacuum aspirator

6. Tilt the T Flask to pool the old media in the corner and CAREFULLY aspirate the liquid, being sure to avoid touching the cells on the flask surface

7. Add the appropriate amount of fresh media to the trapezoidal region, not directly to the bottom of the flask (want to avoid displacing the cells)

   For a T25 flask, use 5mL
   For a T75 flask, use 10mL

8. Replace and tighten the cap; check on cells under microscope and return the flask to the incubator

9. Log feeding in the Cell Culture Log

Subculturing / Passaging Cells

Introduction

Subculturing anchorage-dependent cell lines maintains them at exponential growth phase and ensures that cells do not overcrowd in the dish. Subculturing should occur when cells are roughly 70% to 90% confluent, accourding to ATCC.

NOTE: For this protocol, example volumes are given in red that correspond to use of a T25 flask with a 1:4 dilution ratio. Be sure to adjust these volumes accordingly if a different flask size or ratio is used!

A subcultivation ratio of 1:4 to 1:8 is recommended for CHO-K1 cells

Troubleshooting suggestions can be found on p. 11 of the following document:
https://www.atcc.org/~/media/pdfs/culture%20guides/animcellculture_guide.ashx

Materials

> T Flask with cell culture at 70-90% confluence

> Fresh T Flask

> Trypsin-EDTA solution

> PBS

> Appropriate supplemented culture medium

> Aspirating pipette (x2)

> Pipettes (2mL, 5mL

Procedure

Prepare materials

1. Warm trypsin-EDTA solution, PBS, and complete growth medium to 37C in the bead bath

   *Double check whether supplemented media is labeled 5% or 10%

2. Obtain necessary pipettes for the procedure and place them in the hood along the left-hand side

   Note: Please use 10mL pipettes for volumes of greater than 3mL to balance out pipette usage.

3. Prepare a new flask, labeling it with cell type, passage #, dilution ratio, %FBS in media, date, initials

   Passage # should be noted as (your letter)(passage #) for example: A#3

4. Add appropriate volume of fresh supplemented culture medium and warm to 37C in the incubator

   For T25 flask and 1:4 dilution ratio, add 4mL
   For T25 flask and 1:8 dilution ratio, add 4.375mL
   For T25 flask and 1:10 dilution ratio, add 4.5mL

Rinse

5. Remove culture flask to be subcultured from the incubator; sterilize and bring into the hood

   When sterilizing T Flasks, avoid spraying the cap as it contains an air filter.

6. Carefully aspirate the old cell culture medium from the flask, without disturbing the cells

7. Rinse the cell monolaryer with PBS; rock flask back and forth gently to rinse cells and carefully aspirate

   Volume depends on flask size:
   For a T25 flask, use 5mL
   For a T75 flask, use 10mL

Trypsinize

8. Remove warmed trypsin-EDTA solution from the bead bath, **invert several times** then sterilize and bring into the hood

9. Add 1mL of the trypsin-EDTA solution to the flask, ensure it spreads evenly across the area of the flask bottom

10. Observe cells under an inverted microscope until cell layer is dispersed (5-15min): detached cells will appear rounded and refractile.

    For T25 flask, we have found this takes closer to 5 min.
    To avoid clumping, do NOT agitate the cells by hitting or shaking the flask while waiting for them to detach
    Note: Cells that are difficult to detach may be placed at 37C to facilitate dispersal

11. Add 4mL of complete growth medium to the flask and gently pipette up and down

    To pipette up and down, pull up liquid and then release while rocking T-flask back and forth to rinse cells down the wall of the flask. Try to avoid air bubbles. Repeat 4-5 times.

12. Pull up all liquid (5mL total), transfer to centrifuge tube

    Release liquid along the wall of the tube to avoid bubbling.

13. Place in a balanced centrifuge and spin at 125 x g for 10 minutes

14. Carefully aspirate the supernatant (avoid disturbing the pellet)

15. To resuspend, take 2mL of fresh media and pipette up and down 15-20 times

16. Add remaining liquid (to reach 5mL total); **suck liquid down to its base and release all back into the tube (4-5 times)**

    DO THIS CAREFULLY: pipetting up and down quickly with large volumes could lead to accidental overflow

Subculture

17. Remove pre-warmed culture flask with fresh media from the incubator, sterilize and bring into the hood

18. Divide cells based on prescribed culture ratio and add them to the new flask

    Subcultivation ratio depends on cell type;
    for T25 flask and 1:4 ratio, take 1mL of resuspended cells and deposit in center of new flask
    For a 1:8 ratio, take .625 mL of resuspended cells, deposit in center of new flask
    For a 1:10 ratio, take 0.5mL of resuspended cells, deposit in center of new flask

19. Gently rock flask to disperse cells; check for presence of new cells on microscope

20. Log passaging on Cell Culture Log in Benchling

21. Incubate cultures at 37°C; check cells the following day to ensure they have reattached and are actively growing.

Cryopreservation of Cells

Introduction

Cryopreservation of cells stored below -130C is used to maintain reserves of cell cultures. In addition to acting a back-up supply, properly stored cultures can reduce alterations in or loss of culture characteristics that accumulate over time in most cell lines as they age and evolve.

Materials

> 2 mL screw-capped Cryogenic vials

> Complete cell culture medium containing serum (what %)

> Pipettes

> 15 mL screw-capped centrifuge tubes

> PBS

> Trypsin

> Cryoprotective medium: complete culture medium containing 5% (v/v) dimethyl sulfoxide (DMSO) or 10% (v/v) glycerol

> Trypan blue solution or other vital staining solution for determining the viability of the cells during counting

> Controlled-rate freezing unit

>> Make sure that the labeling system is suitable for (permanent) cryogenic storage

> Hemocytometer

Procedure

Culture selection and examination

1. Prior to freezing, the culture should be maintained in an actively growing state (log phase or exponential growth) to ensure optimum health and good recovery. Ideally, the culture medium should be changed 24 hours prior to harvesting.

2. Check your cell culture for contamination from bacteria, fungi, mycoplasma, and viruses immediately before cryopreservation. In most cases, the results of the contamination screen will be available some time after the cultures are cryopreserved (10 to 14 days). If contamination is confirmed, then destroy the frozen material. It is also important to examine the culture with the unaided eye to look for small, isolated fungal colonies that may be floating at the culture medium-air interface and thus are not easily detected with the microscope.

Cell harvesting

3. The standard protocol routinely used for subculturing your cell cultures can generally be used. See Subculturing / Passaging Cells (https://benchling.com/sahalab/f/fXKV4Brk--protocols/prt-BVTWupZ3-subculturing-passaging-cells/edit). Collect suspended cells in a 15-mL centrifuge tube.

4. Collect the suspended cells in a 15-mL centrifuge tube. Remove and set aside a small sample for cell counting and then spin the remaining cell suspension at approximately 100 x g for 5 minutes to obtain a soft cell pellet. Count the cells using a hemocytometer while the tube is spinning. Use the trypan blue solution to check their viability?

Cryoprotective agents

5. Prepare a freeze medium consisting of complete growth medium and 5% DMSO (catalog no. 4-X).

   Make up freezing media: 60% , 20% FBS, 20% DMSO.

6. Remove and discard the supernatant from the centrifuged cells and resuspend the cell pellet in enough of the cell freezing medium to give a final cell concentration of 1×10^6 to 5×10^6 viable cells/ml. Continue to maintain the cells in culture until the viability of the recovered cells is confirmed.

7. Label the appropriate number of vials with the name of the cell line and the date. Then add 1.0 to 1.8 ml of the cell suspension to each of the vials (depending upon the volume of the vial) and seal.

Cell freezing and storage

8. Allow cells to equilibrate in the freeze medium at room temperature for a minimum of 15 minutes but no longer than 60. This time is usually taken up in dispensing aliquots of the cell suspension into the vials. After 60 minutes, cell viability may decline due to the DMSO.

9. A decrease of –1 to –3°C per minute will usually work for most animal cell cultures. The best way to control the cooling process is to use a programmable electronic freezer unit. Place the vials into a controlled-rate freeze chamber, such as ATCC ACS-6000 (https://www.atcc.org/products/all/ACS-6000.aspx), CoolCell LX, and place the chamber in a -70°C (or colder) mechanical freezer for at least 24 hours. Alternately, use a programmable freezer unit set to cool the cryovials at -1°C per minute until a temperature below -70°C is achieved.

10. Quickly transfer the vials to a liquid nitrogen or -130°C freezer. Frozen material will warm up at a rate of 10°C per minute and cells will deteriorate rapidly if warmed above -50°C. If the transfer cannot be done immediately, the vials can be placed on dry ice for a short time.

11. Record the location and details of the freeze.

12. After 24 hours at -130°C, remove one cryovial, restore the cells in culture, and determine their viability and sterility.

Cleanup Checklist

SUNDAY, 4/7/2019

- ☐ Return all aliquots from hood and bead bath to the correct storage temperature. If a new aliquot was used, mark an "X" on the cap.
    - Trypsin/EDTA at -20C
    - Supplemented media at 4C (cover in foil to protect from light)
    - PBS at room temp
    - FBS at -20C
- ☐ Anything that has contained cells (centrifuge tubes, flasks) must be bleached
    - Add bleach & wait ~20 min; afterward liquids may be poured down the drain, plastics are trash and glass goes in sharps disposal.
- ☐ Throw away BSL trash. Pipettes into sharps container, everything else into BSL trash in the prep room
- ☐ Plug in pipettor to charge
- ☐ Tidy up workspace--throw away other misc. trash, wipe down tabletops
- ☐ Check that microscope, centrifuge are switched off. Turn off lights and close the door behind you.